derivatives is tested by a finite difference scheme. The results are listed in Table 1.

Conclusions

An efficient and practical procedure based on the generalized Schmidt orthogonalization is presented to compute the eigenvector derivatives when repeated eigenvalues exist. The proposed procedure preserves the merits of the published methods but need not solve a high-order linear equation. Furthermore, the new method can be easily implemented on computer. As an example, we computed the eigenvector derivatives of repeated eigenvalues for a cantilever beam and compared the accuracy of the proposed method with a finite difference scheme.

References

[1]Adelman, H. M., and Haftka, R. T., "Sensitivity Analysis of Discrete Structural Systems," *AIAA Journal*, Vol. 24, No. 5, 1986, pp. 823–832.

[2]Nelson, R. B., "Simplified Calculations of Eigenvector Derivatives," *AIAA Journal*, Vol. 14, No. 9, 1976, pp. 1201–1205.

[3]Ojalvo, I. U., "Efficient Computation of Modal Sensitivities for Systems with Repeated Frequencies," *AIAA Journal*, Vol. 26, No. 3, 1988, pp. 361–366.

[4]Mills-Curran, W. C., "Calculation of Eigenvector Derivatives for Structures with Repeated Eigenvalues," *AIAA Journal*, Vol. 26, No. 7, 1988, pp. 867–871.

[5]Dailey, R. L., "Eigenvector Derivatives with Repeated Eigenvalues," *AIAA Journal*, Vol. 27, No. 4, 1989, pp. 486–491.

[6]Shaw, J., and Jayasuriya, S., "Modal Sensitivities for Repeated Eigenvalues and Eigenvalue Derivatives," *AIAA Journal*, Vol. 30, No. 3, 1992, pp. 850–852.

[7]Hou, G. J. W., and Kenny, S. P., "Eigenvalue and Eigenvector Approximate Analysis for Repeated Eigenvalue Problems," *AIAA Journal*, Vol. 30, No. 9, 1992, pp. 2317–2324.

[8]Liu, Z. S., Chen, S. H., Yu, M., and Zhao, Y. Q., "Contribution of the Truncated Modes to Eigenvector Derivatives," *AIAA Journal*, Vol. 32, No. 7, 1994, pp. 1551–1553.

[9]Mills-Curran, W. C., "Comment on 'Eigenvector Derivatives with Repeated Eigenvalues,' " *AIAA Journal*, Vol. 28, No. 10, 1989, p. 1846.

Effects of Geometries, Clearances, and Friction on the Composite Multipin Joints

Seung Jo Kim* and Jin Hee Kim†
Seoul National University,
Seoul 151-742, Republic of Korea

Introduction

PREDICTIONS of strength and failure mode for laminated composite plates with pin-loaded holes are important for structural engineers. The calculations require precise knowledge of the load distribution around the holes. Therefore, precise calculation of contact stresses around the hole, including consideration of unknown contact area, is important.

To date, many investigators have studied the pin-loaded plate problem analytically[1–3] and numerically.[4–10] In the literature, pin elasticity,[3,6] friction,[1–4,6,8] and contact clearance between pin and hole[1,3,4,6–9] have been studied as the important design factors. Also, in the contact area, it is generally accepted that there are two distinct regions: nonslip and slip. But, because of extreme difficulties, only a few papers[3,4,6,8] have included the nonslip region. Furthermore, although several workers[5,7,8,10] have studied the multipin-joint problem, most, except Kim and Kim,[8] considered the frictionless case or only the slip region in the frictional case because of the complexity.

In this Note, an extensive parametric study of composite multipin joints is performed by the penalty finite element method.[7,8] Design parameters, geometric factors, contact clearances, and friction are considered. Pin elasticity is not considered here since previous work[3] has shown that it is not as important as the other factors. To investigate anisotropic behavior of laminated composite plates, two representative quasi-isotropic laminates, $[0/\pm 45/90\,\text{deg}]_s$ and $[0_2/\pm 45\,\text{deg}]_s$, are used in the analysis. For the multipin-joint models, two pins in series and two in parallel are examined. Geometric factors include width of the plate (W), distance from upper edge of the plate to the hole center (E), and distance between the pins (G). Results include contact distributions for each case and the pin-loading analysis for two pins in series.

Description of the Problem

To analyze the stress around the holes in a pin-loaded anisotropic plate, the problem is idealized as a two-dimensional plane stress problem, where the pin is assumed to be rigid.

The pin-joint problem is naturally formulated as the frictional contact problem. A general class of contact problem with friction is characterized by the following set of equations and inequalities:

$$\begin{aligned} \sigma_{ij,j} + f_i = 0 \quad &\text{in} \quad \Omega \\ u_i = 0 \quad &\text{on} \quad \Gamma_D \\ \sigma_{ij} n_j = t_i \quad &\text{on} \quad \Gamma_F \end{aligned} \tag{1}$$

and on Γ_C
if $u_n - s < 0$

$$\sigma_n = 0, \qquad \sigma_T = 0 \tag{2}$$

if $u_n - s = 0$

$$\sigma_n < 0, \qquad u_T = 0 \qquad \text{if } |\sigma_T| < \mu|\sigma_n| \tag{3}$$

$$\sigma_n < 0, \qquad u_T = -\nu\sigma_T \qquad \text{if } |\sigma_T| = \mu|\sigma_n| \tag{4}$$

where Ω is a smooth domain and Γ_D is a displacement-prescribed boundary, Γ_F is a force-prescribed boundary, Γ_C is a candidate contact boundary, and μ is the friction coefficient. These systems of equations and inequalities describe a class of the signorini problems that obey the Coulomb friction law. As mentioned in the preceding section, the contact region can be divided into two distinct regions: the nonslip region is characterized in Eq. (3), and the slip region is characterized in Eq. (4).

Solution Procedure

To calculate contact stresses around the hole, the penalty finite element method[7,8] is used. For the calculation, the following three procedures are performed. First, the nonfrictional normal contact stress is calculated. In this stage, the extended interior penalty technique is used. For an iterative method, the standard Newton–Raphson scheme is used. Second, utilizing previous nonfrictional normal contact stress, the frictional contact problem with known normal contact stress is solved. In this stage, a regularization procedure for the friction term is performed and a successive tangent stiffness scheme is used for the iteration. Third, frictional force obtained in the second stage is added to total external force, and the equilibrium state is searched again. Until the global equilibrium state is reached, the previous three stages are repeated. For the global convergence criterion, relative error of normal stress is used. Details of the solution to the contact problem can be found in Refs. 7 and 8.

Numerical Results

Two representative cases of real multipin joints are analyzed: the plate with two holes in series and the plate with two holes in parallel. The two quasi-isotropic laminates considered here have stacking sequences of $[0/\pm 45/90\,\text{deg}]_s$ and $[0_2/\pm 45\,\text{deg}]_s$. The material

Received Oct. 31, 1994; revision received Oct. 10, 1995; accepted for publication Oct. 30, 1995.

*Professor, Department of Aerospace Engineering. Member AIAA.
†Graduate Research Assistant, Department of Aerospace Engineering. Member AIAA.

properties of graphite/epoxy composite (Gr/Ep)[3] are taken. For convenience, the friction coefficient μ is assumed to be constant on the contact boundary.

To evaluate the effects of several factors, the contact stresses are computed for two clearances levels, two friction levels, and two different geometric dimensions. Two clearance levels, $\lambda = 0$ and 0.1%, are used. The nondimensionalized clearance λ is defined as the ratio between contact clearance and the radius of the hole $[\lambda = (R_h - R_p)/R_h]$. The case of $\lambda = 0$ represents the ideal perfect fit. The case of $\lambda = 0.1\%$ is used to simulate the actual circumstances in the pin-joint area. Two friction levels, $\mu = 0$ and 0.2, are used, where the case of $\mu = 0$ represents ideal frictionless slip and the case of $\mu = 0.2$ represents the real friction coefficient of steel on Gr/Ep.[3] Also, the analyses are performed for two different values for each geometric factor.

All contact stresses are normalized by the average bearing stress $S(S = P/Dt)$, where P is the total applied force, D the diameter of the hole, and t the thickness of the plate.

Two Pins in Series

The mesh system from Ref. 8 is used for the analysis. Half the plate with two holes in series is modeled by 568 four-node linear elements with 648 nodes, by utilizing symmetry.

In Fig. 1, the results of $[0_2/\pm 45\ \text{deg}]_s$ laminate are shown when $P = 8000$ N, $\lambda = 0$, and $\mu = 0.2$. Similar to the contact area for a single hole,[8] the contact area with friction is wider than that without friction. Also, the contact stress distribution and the location of the maximum contact stress vary with friction. Our computations show that the lower pin experiences more load but less contact area than the upper pin in the $[0/\pm 45/90\ \text{deg}]_s$ laminate, but the lower pin experiences more load and wider contact area in the $[0_2/\pm 45\ \text{deg}]_s$ laminate with the same geometry.

When the clearances of two pins are different from each other, the results are very different from those of perfect-fit cases. In Table 1, pin loadings for various clearances are shown. When the clearance of the lower pin is larger than that of the upper pin, the upper pin has more load and vice versa. Note that friction has little influence on the pin loading, as shown in Table 1. Friction slightly increases the pin loading of the lower pin.

Table 1 Pin loadings with variation of clearances

Case[a]		Frictionless case, N Upper	Frictionless case, N Lower	Frictional case, N Upper	Frictional case, N Lower
I	A[b]	2926	5074	2866	5134
	B[c]	3008	4992	2938	5062
II	A	3186	4814	3170	4830
	B	3228	4772	3204	4796
III	A	2762	5238	2706	5294
	B	2830	5170	2756	5244

[a]I) both 0%; II) upper 0.1%, lower 0.2%; and III) upper 0.2%, lower 0.1%.
[b]$A = [0/\pm 45/90\ \text{deg}]_s$.
[c]$B = [0_2/\pm 45\ \text{deg}]_s$.

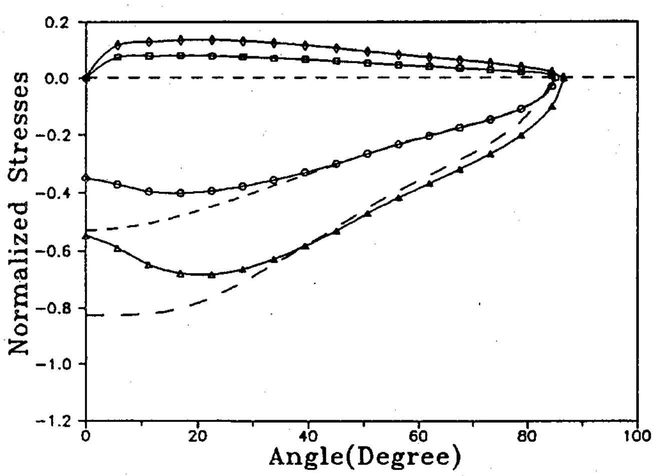

Fig. 1 Contact stress distribution of $[0_2/\pm 45\ \text{deg}]_s$ laminate in the case of two pins in series: - - - -, nonfriction (upper); -⊖-⊖-⊖-, friction normal (upper); -⊟-⊟-⊟-, tangential (upper); — — —, nonfriction (lower); -△-△-△-, friction normal (lower); and -◇-◇-◇-, tangential (lower).

Table 2 Pin loadings with variation of W

Case[a]		Frictionless case, N Upper	Frictionless case, N Lower	Frictional case, N Upper	Frictional case, N Lower
I	A[b]	2930	5070	2886	5114
	B[c]	2992	5008	2933	5067
II	A	2120	5880	2044	5956
	B	2400	5600	2316	5684

[a]I) $W/R = 16$; II) $W/R = 8$.
[b]$A = [0/\pm 45/90\ \text{deg}]_s$.
[c]$B = [0_2/\pm 45\ \text{deg}]_s$.

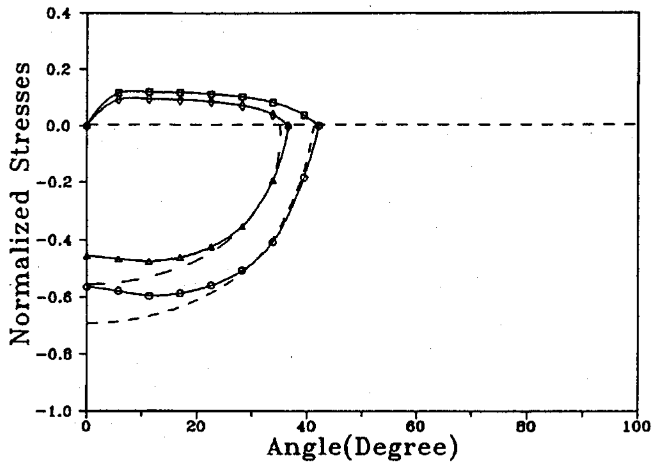

Fig. 2 Contact stress distribution in upper pin of the $[0/\pm 45/90\ \text{deg}]_s$ laminate for variation of W in the case of two pins in series: case I) $W/R = 16$; and case II) $W/R = 8$: - - - -, nonfriction (case I); -⊖-⊖-⊖-, friction normal (case I); -⊟-⊟-⊟-, tangential (case I); — — —, nonfriction (case II); -△-△-△-, friction normal (case II); and -◇-◇-◇-, tangential (case II).

The results in the upper pin when the width of the plate W is varied are shown in Fig. 2 when $P = 8000$ N, $\lambda = 0.1\%$, and $\mu = 0.2$ in both pins and when the $[0/\pm 45/90\ \text{deg}]_s$ laminate is used. Contrary to the results obtained with a single hole, the effect of the width of the plate on contact stress distributions is notable. As the width of the plate becomes narrower, the upper pin experiences less load and narrower contact area. So, the lower pin experiences more load and wider contact area. Further, the load path also changes and a very different loading for each pin can be expected. In Table 2, the pin loadings with variation of W are shown. It can be stated from the table that the variation of W is important in determining the load path of the pin-joint structure where there are two pins in series. In this case, friction slightly increases the pin loading of the lower pin.

Our computations show that the effect of the distance between two pins is that a smaller distance between two pins increases the load on the upper pin and slightly decreases the contact area. Regarding the effect of the distance from the upper edge to upper pin, when the upper pin moves toward the upper edge of the plate, the upper pin experiences less load and the lower pin more load.

We concluded that several factors, such as clearances, friction, and geometry, play important roles in determining the load path of a pin-joint structure. But, although friction is the most important factor for calculating the contact stress distribution and the failure characteristic, the friction effect is not important when calculating only the amount of pin loading of each pin. Note also that the $[0_2/\pm 45\ \text{deg}]_s$ laminate usually experiences more load in the upper pin than the $[0/\pm 45/90\ \text{deg}]_s$ laminate. But, when G/R or E/R becomes smaller, the former laminate has less load in the upper pin than the latter laminate.

Two Pins in Parallel

For the analysis of two holes in parallel, the mesh system from Ref. 8 is used for the analysis. Half the plate with two holes in

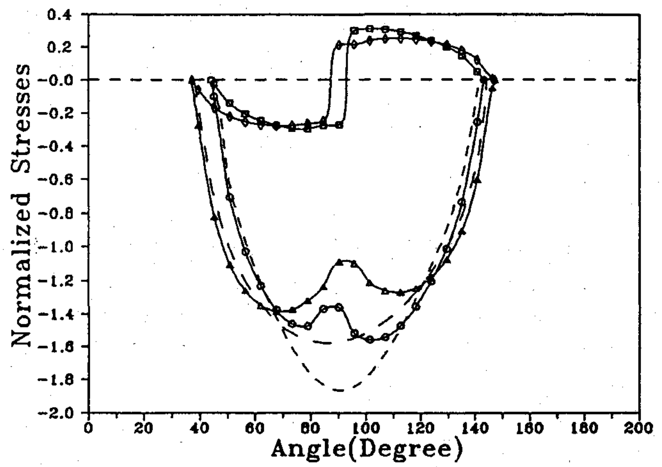

Fig. 3 Contact stress distribution of $[0_2/\pm 45\ \mathrm{deg}]_s$ laminate for variation of E in the case of two pins in parallel: case I) E/R = 6; and case II) E/R = 3: - - - -, nonfriction (case I); -⊖-⊖-⊖-, friction normal (case I); -⊟-⊟-⊟-, tangential (case I); — — —, nonfriction (case II); -△-△-△-, friction normal (case II); and -◇-◇-◇-, tangential (case II).

parallel is discretized by 546 four-node linear elements with 613 nodes by utilizing symmetry. In Fig. 3, the results for two values of distance between the upper edge of the plate to the center of hole E are shown for the $[0_2/\pm 45\ \mathrm{deg}]_s$ laminate. As E becomes smaller, maximum normal contact stress is reduced and the point of sign change of tangential stress is located outward from the symmetric axis of the plate. Also, a wider contact area is found as E becomes smaller. Also, our computations show the following effects of distance from the symmetric axis of the plate to the hole G: both contact areas are almost the same, but the maximum normal contact stress moves toward the symmetric axis of the plate as G becomes smaller.

The results indicate the importance of geometric factors in the design of pin-joint structures. In all cases, $P = 8000$ N, $\lambda = 0.1\%$, and $\mu = 0.2$ are assumed.

Conclusions

This study investigated the parametric behavior of multipin joints of laminated composite plates. Clearances, friction coefficients, and geometric factors are considered as design parameters for the analysis. Using the penalty finite element method, the pin-joint problems are solved.

Through extensive parametric study, the following can be concluded: Friction and clearance have a significant influence on the distribution and the maximum value of the contact stresses. Friction changes the location of the maximum contact stresses and increases contact area. Clearance affects contact area and the maximum contact stress. Note that geometric factors also significantly influence the distribution of contact stresses. These factors change the location of maximum contact stress and contact area. Also, pin loadings are changed significantly with variation of the above mentioned parameters in case of two pins in series. These findings will be useful for the design of composite structures by the aerospace industry.

References

[1]Oplinger, D. W., Gandhi, W., and Gandhi, K. R., "Stress in Mechanically Fastened Orthotropic Laminates," *2nd Conference of Fiber Composites in Flight Vehicle Design*, 1974, pp. 813–841.

[2]De Jong, T., "The Influence of Friction on the Theoretical Strength of Pin-Loaded Holes in Orthotropic Plates," Rept. LR-350, Dept. of Aerospace Engineering, Delft Univ. of Technology, Delft, The Netherlands, 1982.

[3]Hyer, M. W., Klang, E. C., and Cooper, D. E., "The Effect of Pin Elasticity, Clearance and Friction on the Stresses in a Pin-Loaded Orthotropic Plate," *Journal of Composite Materials*, Vol. 21, 1987, pp. 190–206.

[4]Wilkinson, T. L., Rowlands, R. E., and Cook, R. D., "An Incremental Finite Element Determination of Stresses Around Loaded Holes in Wood Plates," *Computers and Structures*, Vol. 14, Nos. 1, 2, 1981, pp. 123–128.

[5]Chang, F. K., Scott, R. A., and Springer, G. S., "Strength of Mechanically Fastened Composite Joints," *Journal of Composite Materials*, Vol. 16, 1982, pp. 470–494.

[6]Yogeswaren, E. K., and Reddy, J. N., "A Study of Contact Stresses in Pin-Loaded Orthotropic Plates," *Computers and Structures*, Vol. 30, No. 5, 1988, pp. 1067–1077.

[7]Kim, S. J., and Kim, J. H., "Finite Element Analysis of Laminated Composites with Contact Constraint by Extended Interior Penalty Method," *International Journal for Numerical Methods in Engineering*, Vol. 36, No. 20, 1993, pp. 3421–3439.

[8]Kim, S. J., and Kim, J. H., "Finite Element Analysis of Laminated Composite Plates with Multi Pin Joints Considering Friction," *Computers and Structures*, Vol. 55, No. 3, 1995, pp. 507–514.

[9]Naik, R. A., and Crews, J. H., Jr., "Stress Analysis Method for a Clearance-Fit Bolt Under Bearing Loads," *AIAA Journal*, Vol. 24, No. 8, 1986, pp. 1348–1353.

[10]Yang, L., and Ye, L. Y., "Study of the Behavior of a Composite Multi-Bolt Joint," *Computers and Structures*, Vol. 34, No. 3, 1990, pp. 493–497.

New Method for Deriving Eigenvalue Rate with Respect to Support Location

Zhong-sheng Liu* and Hai-chang Hu†
Jilin University of Technology,
Changchun 130022, People's Republic of China
and
Da-jun Wang†
Peking University,
Beijing 100871, People's Republic of China

I. Introduction

EIGENVALUE rate with respect to cross-sectional variables and shape variables is of importance in design of structural vibrational systems and, thus, attracts much attention in the research fields.[1–3] Though eigenvalue rate with respect to the cross-sectional variables has been widely and deeply investigated, eigenvalue rate with respect to the shape variables is less evolved. Very recently, Wang[4] used the classical normal modal method to derive the formulas of eigenvalue rate with respect to in-span support; Hou and Chuang[5] used the material derivative method to derive the formulas of eigenvalue rate with respect to in-span support. Their results with the beam as an example show that the eigenvalue rate with respect to in-span support location is proportional to the slope of the corresponding mode shape and the support reaction force. In this Note, the authors present a new method to derive the formulas of eigenvalue rate with respect to in-span support location using the generalized variational principle of the Rayleigh quotient. Following the ideas of this Note, the eigenvalue rate, with respect to such variables as location of discrete or continuous in-span supports, the location of concentrated mass, location of elastic support, and location of a substructure, can be derived without any conceptual difficulties. At the end of this Note, a numerical comparison is given to illustrate the application of the method presented.

II. Problem Definition

For the sake of simplicity, let us take a beam, shown in Fig. 1, as an example to illustrate the new method for deriving the formulas of eigenvalue rate with respect to in-span support location. The beam

Received Jan. 21, 1995; revision received June 12, 1995; accepted for publication June 14, 1995.

*Professor, Department of Mechanics; currently Visiting Professor, Department of Mechanical Engineering, University of California, Berkeley, Berkeley, CA 94720.

†Professor, Department of Mechanics.